# Simultaneous Tamper-less MR Elastography and Diffusion Tensor Imaging of the Human Brain

Kulam Najmudeen Magdoom[1,2,3], Joelle E Sarlls[4], Alexandru V Avram[1], and Peter J Basser[1]
[1]Eunice Kennedy Shriver National Institute of Child Health and Human Development, Bethesda, MD, United States, [2]The Military Traumatic Brain Injury Initiative (MTBI2), Uniformed Services University of the Health Sciences, Bethesda, MD, United States, [3]The Henry M Jackson Foundation for the Advancement of Military Medicine (HJF) Inc., Bethesda, MD, United States, [4]National Institute of Neurological Disorders and Stroke, Bethesda, MD, United States

## Synopsis

**Keywords:** Elastography, Neurofluids

**Motivation:** Conventional *in vivo* brain MRE is challenging, requiring an external tamper, which can be expensive, difficult to operate, and inefficient given the mechanical shielding of the skull.

**Goal(s):** To develop a robust method to simultaneously measure both the shear modulus, and the diffusion tensor fields throughout the brain using pulsations from the heart.

**Approach:** We simultaneously measure both the displacement and diffusion tensor fields by cardiac gated displacement-encoded acquisitions.

**Results:** The DT parameters vary significantly throughout the cardiac cycle. The shear modulus maps show white matter is stiffer than gray matter. Differences in stiffness across various white matter tracts were also observed.

**Impact:** This study could facilitate the use of intrinsic brain tissue motion induced by cardiac pulsations to diagnose subtle neurological diseases.

## Introduction

MR elastography (MRE) [1] and diffusion tensor imaging (DTI) [2] have transformed radiology, however their potential in the brain is not yet fully realized. A primary challenge in brain MRE is the attenuation of externally induced mechanical waves by the skull. An external tamper can also be costly, difficult to operate, and may not be suitable for all patient cohorts. Subtle changes in DT parameters that occur in disease are often confounded by intrinsic brain pulsations [3], and a straightforward comparison of diffusion and mechanical properties is challenging due to inter-scan subject motion.

The goal of this work is to simultaneously perform DTI and MRE by using the deformations caused by the internal pressure pulse wave from the heart entering the cranium instead of via an external tamper. While intrinsic MRE has been attempted in several previous studies [4, 5], they involve computationally intensive finite element method (FEM) reconstructions and/or use stimulated echo displacement encoding (DENSE), which can be difficult to implement. Moreover, they do not provide concomitant diffusion tensor maps. In this study, we use spin echo phase contrast MRI with sub- voxel displacement sensitivity to measure subtle brain tissue motion within a heartbeat. We then use this data to simultaneously map both the diffusion tensor associated with the brain motions as a function of the cardiac phase, and the shear modulus map with fast direct inversion of the equations of motion.

## Methods

MRI data was acquired in three healthy young adults on a 3T scanner (Prisma, Siemens Healthineers) with 80 mT/m peak gradient strength and a 200 T/m/s slew rate using 20-channel coil. Whole-brain displacement encoded MRI data was acquired along the six directions of the icosahedron at b = 350 s/mm$^2$ and $v_{enc}$ = 0.4 mm/s along with a b = 0 s/mm$^2$ scan using the following parameters: δ\Δ = 7\48 ms, FOV=210 x 210 x 120 mm, GRAPPA factor = 2, TR\TE = 5,600\71 ms, NEX = 144, and a 2 mm isotropic spatial resolution. Narrow gradient pulses with long diffusion time were chosen to increase flow sensitivity while maintaining adequate diffusion sensitivity [6]. The pulse-oximeter signal and MRI triggers were simultaneously recorded using a Biopac System (Biopac, Goleta, CA, USA) for retrospective gating.

Linear phase errors arising from eddy currents, rigid body motion, etc., were removed using linear regression. The $\Delta B_0$-induced geometric distortion is corrected using FSL's topup software [7]. The displacement-encoded images were then segmented into ten different bins each 100 ms long covering the entire cardiac cycle. Multiple repetitions of the data acquired in each bin for a given direction were utilized to reject inconsistent phase measurement in each voxel. The 3D displacement vector and the diffusion tensor fields were concurrently estimated from the phase and magnitude signals, respectively, using linear regression. The displacement vector field is Fourier transformed in time to estimate its amplitude at the cardiac frequency (i.e., ~1 Hz) which was subjected to a Helmholtz decomposition [8] with a positivity constraint to estimate the voxel wise isotropic shear modulus.

## Results and Discussion

The real part of the displacement vector oscillating at the cardiac frequency is shown in Figure 1. The funnel shaped motion of the brain along its superior-inferior axis, well documented in the literature [9, 10], is captured in these plots. The kinematic components of the filtered displacement field which reflect tissue mechanical properties, are shown in Figure 2. We observe that the divergence and curl are both non-zero and heterogeneous in the brain parenchyma. The diffusion tensor maps are shown in Figure 3 throughout the cardiac cycle. Changes in mean diffusivity (MD) and fractional anisotropy (FA) were observed in ventricles from increased CSF flow during systole, and in the brain parenchyma likely due to intravoxel phase dispersion resulting from local deformations [11, 12]. The estimated shear modulus in the brain is shown in Figure 4 along with MD and FA maps for comparison. The shear modulus is heterogeneous with white matter being stiffer than gray matter as shown in high-frequency MRE studies [13]. Differences in stiffness among various white matter pathways were also visible. The brain appears ultrasoft at the cardiac frequency given the very long waves (~15-20 cm) observed.

## Conclusion

We have demonstrated a method to map the shear modulus and diffusion tensor fields simultaneously in live human brain without an external tamper using spin echo displacement encoding. The results show the white matter stiffer than gray matter and cardiac gating may be necessary in DTI acquisitions when aiming to measure very subtle changes in diffusion properties that may occur in disease.

## Acknowledgements

This study was supported by the Intramural Research Program of the Eunice Kennedy Shriver National Institute of Child Health and Human Development and the National Institute of Neurological Diseases and Stroke. This work was also partly funded by the Department of Defense in the Military Traumatic Brain Injury Initiative under award, HU0001-22-2-0058. The authors have no conflicts of interest to disclose. The views, information or content, and conclusions presented do not necessarily represent the official position or policy of, nor should any official endorsement be inferred on the part of, the Uniformed Services University, the Department of Defense, the U.S. Government or the Henry M. Jackson Foundation for the Advancement of Military Medicine, Inc.

## References

1. Muthupillai, R., et al. "Magnetic resonance elastography by direct visualization of propagating acoustic strain waves." science 269.5232 (1995): 1854-1857.

2. Basser, Peter J., James Mattiello, and Denis LeBihan. "MR diffusion tensor spectroscopy and imaging." Biophysical journal 66.1 (1994): 259-267.

3. Chung, S., Courcot, B., Sdika, M., Moffat, K., Rae, C., & Henry, R. G. (2010). Bootstrap quantification of cardiac pulsation artifact in DTI. Neuroimage, 49(1), 631-640.

4. Weaver, John B., et al. "Brain mechanical property measurement using MRE with intrinsic activation." Physics in Medicine & Biology 57.22 (2012): 7275.

5. Burman Ingeberg, M., Van Houten, E., & Zwanenburg, J. J. M. (2023). Estimating the viscoelastic properties of the human brain at 7 T MRI using intrinsic MRE and nonlinear inversion. Human brain mapping, 44(18), 6575–6591. https://doi.org/10.1002/hbm.26524

6. Magdoom, K. N., Zeinomar, A., Lonser, R. R., Sarntinoranont, M., & Mareci, T. H. (2019). Phase contrast MRI of creeping flows using stimulated echo. Journal of Magnetic Resonance, 299, 49-58.

7. Andersson, Jesper LR, Stefan Skare, and John Ashburner. "How to correct susceptibility distortions in spin-echo echo-planar images: application to diffusion tensor imaging." Neuroimage 20.2 (2003): 870-888.

8. Sinkus, R., et al. "Imaging anisotropic and viscous properties of breast tissue by magnetic resonance-elastography." Magnetic Resonance in Medicine: An Official Journal of the International Society for Magnetic Resonance in Medicine 53.2 (2005): 372-387.

9. Poncelet, B. P., Wedeen, V. J., Weisskoff, R. M., & Cohen, M. S. (1992). Brain parenchyma motion: measurement with cine echo-planar MR imaging. Radiology, 185(3), 645-651.

10. Sloots, J. J., Biessels, G. J., & Zwanenburg, J. J. (2020). Cardiac and respiration-induced brain deformations in humans quantified with high-field MRI. Neuroimage, 210, 116581.

11. Nevo, U., Özarslan, E., Komlosh, M. E., Koay, C. G., Sarlls, J. E., & Basser, P. J. (2010). A system and mathematical framework to model shear flow effects in biomedical DW-imaging and spectroscopy. NMR in Biomedicine, 23(7), 734-744.

12. Reese, T. G., Wedeen, V. J., & Weisskoff, R. M. (1996). Measuring diffusion in the presence of material strain. Journal of Magnetic Resonance, Series B, 112(3), 253-258.

13. Hiscox, Lucy V., et al. "Magnetic resonance elastography (MRE) of the human brain: technique, findings and clinical applications." Physics in Medicine & Biology 61.24 (2016): R401.

## Figures

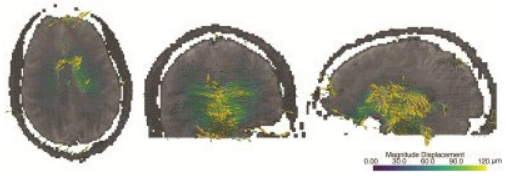

Figure 1: 3D vector plots showing the real part of the frequency-filtered intrinsic displacement field in three orthogonal planes in the brain oscillating at the cardiac frequency. The length of each vector is scaled by its magnitude and colored accordingly. The magnitude MRI images were used as underlay for anatomical reference. Vectors pointing into the page especially in the anterior and posterior portions of the brain regions are not clearly visible. The funnel like motion of the brain is accurately captured throughout the imaging volume.

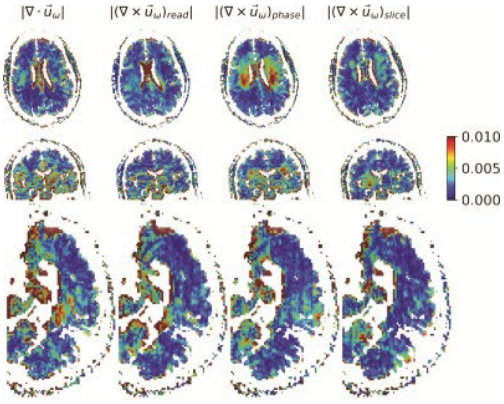


Figure 2: The magnitude of the kinematic components of the filtered displacement vector field (i.e., divergence and curl) in the brain which determine its mechanical properties are shown for the three orthogonal planes. In patient coordinates, the read direction is right-left, phase direction is anterior- posterior, and slice is foot-head respectively. The CSF filled regions are masked out based on their mean diffusivity values for scaling purposes. It can be observed that both the divergence and curl components are heterogeneous throughout the brain albeit smaller in magnitude.

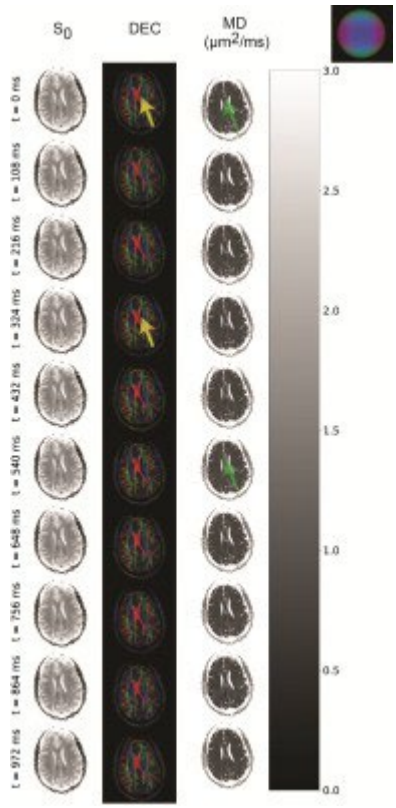


Figure 3: DTI derived maps at various segments throughout the cardiac cycle. The maps include the $T_2$ weighted image ($S_0$), direction encoded color (DEC) map along with the color sphere, and mean diffusivity (MD). Several changes can be observed in these maps across the various segments. For example, changes are observed in the isotropic CSF filled ventricles as shown by the yellow arrows in DEC maps aligning with the CSF flows. Subtle changes in MD are also observed where an elevated value is observed in the corpus callosum at the middle of the cardiac cycle as shown by the green arrows.

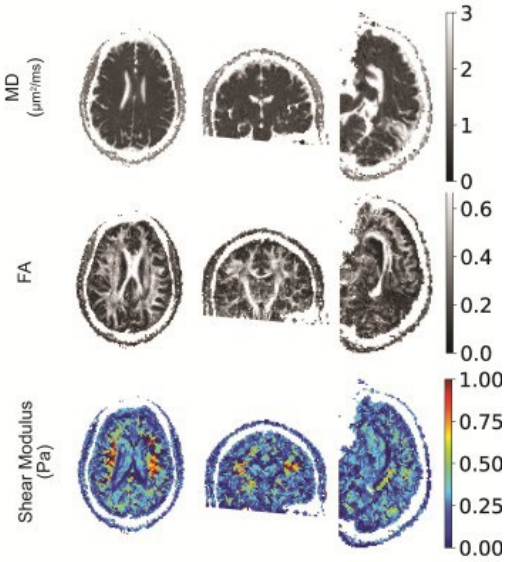


Figure 4: Diffusion and mechanical property maps for three orthogonal slices in the brain. The MD and FA maps in the middle of the cardiac cycle are compared with the shear modulus map. It can be observed that while MD is uniform in the brain parenchyma, the shear modulus is heterogeneous with white matter stiffer than gray matter. Differences in stiffness among various white matter tracts are also visible, the splenium of corpus callosum appears slightly stiffer than the genu and body, and the corona radiata appears much stiffer than the corpus callosum.